Hydrological Processes
Hydrol. Process. **12**, 923–941 (1998)

Deciphering large landslides: linking hydrological, groundwater and slope stability models through GIS

Daniel J. Miller[1,2]* and Joan Sias[2]

[1]*M2 Environmental Services, 4232 5th Ave NW, Seattle, WA 98107, USA*
[2]*Earth Systems Institute, 1314 NE 43 St., Suite 207, Seattle, WA 98105, USA*

Abstract:

Large landslides can deliver substantial volumes of sediment to river channels, with potentially adverse consequences for water quality and fish habitat. When planning land use activities, it is important both to consider the risks posed by landslides and to account for the effects of land use on rates of landslide movement. Of particular interest in the Pacific Northwest are the effects of timber harvest in groundwater recharge areas of landslides. Because of variability between sites, and variability over time in precipitation and other natural environmental factors affecting landslide behaviour, empirical data are usually insufficient for making such determinations. We describe here the use of simple numerical models of site hydrology, groundwater flow and slope stability for estimating the effects of timber harvest on the stability of the Hazel Landslide in northwestern Washington State. These effects are examined relative to those of river bank erosion at the landslide toe. The data used are distributed in time and space, as are the model results. A geographical information system (GIS) provides an efficient framework for data storage, transfer and display. Coupled with process-based numerical models, a GIS provides an effective tool for site-specific analysis of landslide behaviour.

KEY WORDS landslides; GIS; hydrology; groundwater; slope stability; forest hydrology

INTRODUCTION

Large landslides involve a broad range of mass-wasting processes. Even a single landslide, or landslide complex, can exhibit a variety of behaviours and respond to a variety of environmental factors, some of which may be removed from the landslide itself. Factors affecting groundwater flow, for example, may be distributed over a large area. These issues present a recurring challenge to natural resource managers in areas of active or potential landslide activity. Simple avoidance of landslide-prone areas can be an expensive option, and may not be necessary if land use activities will have no influence on landslide behaviour.

Characterizing the effects of distributed land use on landslide activity is traditionally an empirical endeavour (e.g. Sidle *et al.*, 1985). To assess the effects of forest management on landslide occurrence, for example, Washington State has implemented a procedure (WFPB, 1995) that relies on correlations between landslide rates (e.g. number of landslides per square kilometre per year) and forestry activities (e.g. timber harvest and road construction). This procedure works satisfactorily for small, shallow landslides. Unfortunately, large landslide complexes are not as amenable to empirical categorization. For example, timber harvest can increase groundwater levels over a period of years (see Hammond *et al.*, 1992 for a review) with consequent increases in rates of mass movement (Swanston *et al.*, 1988). Cause and consequence may be separated in both space and time. The diversity of the interacting factors potentially affecting

* Correspondence to: Daniel J. Miller, M2 Environmental Services, 4232 5th Ave NW, Seattle, WA 98107, USA.

CCC 0885–6087/98/060923–19$17·50

Received 30 May 1997
Revised 15 September 1997
Accepted 20 November 1997

the behaviour of large landslides confounds attempts to find simple relationships between land use and landslide activity.

Careful monitoring may reveal apparent connections between forestry activities and mass movement rates (Swanston *et al*., 1988). However, monitoring programmes require funding, perhaps over the course of many years. Extended funding is difficult to obtain without some indication that the costs will eventually pay off. Moreover, to find the link between forest land management and landslide activity, or a lack thereof, requires that some forestry activity is actually performed, an experiment that may not be allowed if the potential consequences of accelerated mass wasting are considered too dire.

An alternative is first to simulate the experiment numerically, a feat that has become feasible only with the advent of geographic information systems (GIS). With GIS, simple process-based models using digital data can be applied over broad areas (Dietrich *et al*., 1995; Miller, 1995). Various scenarios can be examined, with parameter values altered to reflect a proposed land use. The results offer an estimate of landslide response with which to evaluate the risk of actually performing the land use experiment, and can guide efforts at data collection and monitoring.

These methods can also be used to formulate hypotheses to test and improve our understanding of the processes active within a large landslide. Model response to a change in any of the pertinent variables (groundwater recharge, for example) can isolate the role of various factors that affect slope stability. Spatially distributed data allow explicit prediction of the spatial pattern of slope response to such changes. By simulating an historical change in any of the driving variables, we predict a landslide response to compare with what has been observed.

The key to this approach is calculation of a response to a change in some controlling variable. We find that attempts to predict slope stability directly, i.e. a factor of safety, meet with less success. The reason is that the data available for such broad application of a slope stability model are very limited. We lack, for example, any geotechnical tests, so that rock and soil property values are constrained only by the range of values reported for similar rock and soil types. The change in the factor of safety calculated for a change in any model variable is a more robust predictor of slope sensitivity to environmental perturbations than the 'factor of safety' values themselves.

Here, we illustrate the use of process-based models implemented through a GIS with an analysis of the Hazel Landslide, a large landslide complex in glacio lacustrine sediments adjacent to the Stillaguamish River in north-western Washington, USA. Sediment shed from this landslide has posed a chronic threat to an important fishery for decades. Upslope areas are managed for timber production. This study was motivated by concerns that timber harvesting within the groundwater recharge area of the landslide could increase groundwater flow, and consequently increase sediment flux from the landslide. Previous studies have highlighted the potential importance of groundwater flow to the landslide (Shannon and Associates, 1952; Benda *et al*., 1988), but were unable to quantify its role relative to other factors (WDNR, 1996).

For this analysis, we were asked to estimate the potential effects of clear-cut timber harvesting in areas upslope of the landslide (no harvests are proposed on the landslide itself) relative to the effects of bank erosion of the landslide toe. The data available were: a 1 : 4800-scale topographic map of the area; time-series of precipitation and temperature from a regional weather station; and field estimates of stratigraphic contact and surface seep locations. The stratigraphy consists of a thick sequence of glaciofluvial sediments (primarily sand) overlaying lacustrine silts and clays. Surface seeps are found year-round, emerging at the sand–clay contact in many places. Some of these seeps are associated with areas of activity on the Hazel Landslide. The aerial distribution and flux from the seeps were mapped in autumn (the end of the dry season) and spring (the end of the wet season). The topographic and field-mapped data were digitized and used with simple models to estimate: (1) recharge to groundwater; (2) the aerial pattern of groundwater flow (assuming the outwash deposits act as an unconfined aquifer); and (3) slope stability over the area of the landslide. Data transfer and display were accomplished within a GIS. We used the calculated water table to estimate the extent of the groundwater recharge area to the landslide and then examined model responses to: (1) clear-cut timber harvesting of the groundwater recharge area; (2) bank erosion of the landslide toe, and; (3) incision of

small stream channels draining the body of the landslide. The results indicate large spatial variability in the magnitude of the response to each of these changes, with patterns of response unique to each process. Compared with patterns of landslide activity observed in historical sequences of aerial photographs and in the field, these results offered hypotheses to explain landslide behaviour and provided insight that guided land management decisions.

Our modelling strategy was dictated in part by the characteristics of the Hazel Landslide. Although the techniques presented here have much broader applicability, it is useful to describe them in the context of their application in this case, so we start below with a description of the site.

Site characteristics

The Hazel Landslide sits at the south-east end of the Whitman Bench (Figure 1), a large terrace remnant composed of lacustrine clays underlying glaciofluvial outwash, a stratigraphic sequence common in valleys draining the Cascade Mountains west to Puget Sound (Tabor *et al.*, 1988; Booth, 1989). Extensive fluvial incision of these deposits following the Vashon stade of the Fraser Glaciation (12 000 years) created conditions conducive to mass wasting. Morphology indicative of large, deep-seated landsliding within these deposits is common throughout this region. Although most such landslides appear to be dormant, several recently and currently active deep-seated landslides, such as the Hazel Landslide, attest to the continuing potential for mass movement of this material (e.g. Thorsen, 1989). Several large, post-glacial slump blocks (currently dormant) scallop the margins of the Whitman Bench. As shown in Figure 1, the Hazel Landslide is contained within one of these blocks and the surrounding topography indicates adjacent slumps to the west and to the north.

The climate at Hazel is maritime, with cool, humid winters and dry summers. Annual average rainfall at the nearest weather station (the US Forest Service ranger station in Darrington, Washington; 17·6 kilometres to the east) is 2250 mm per year (1931–1994), with 84% of rainfall occurring from October to April. Average January and July air temperatures are 2·1 °C (36 °F) and 19·5 °C (67 °F), respectively. We assume 24-hour precipitation at Hazel is 78% that at Darrington (Wolff *et al.*, 1989) and that there is equivalence of air temperature at the two sites. Digital meteorological data were available for the period 1931–1994.

In addition to geographical proximity, there are other relevant similarities between Hazel and Darrington that further justify the suitability of these data. These include: elevation (the climate station is located at 500 feet; the toe of the landslide and the Whitman Bench are at elevations of about 300 and 800 feet, respectively); aspect (both are oriented to the south-west); exposure to frontal weather; and characteristics of upwind terrain — with respect to both topography and vegetation. On the other hand, the meteorological data are collected over a clearing, and therefore may not be very representative of meteorological conditions over a forest, quite possibly introducing a bias towards overestimation of forest (but not clear-cut) evapotranspiration (Pearce *et al.*, 1980).

The Hazel Landslide exhibits several types of activity (Figure 2; Shannon and Associates, 1952; Benda *et al.*, 1988; Miller and Sias, 1997). The most spectacular are slumps that occur in steep scarps along the river edge and evolve into debris avalanches (following the classification of Varnes, 1978). These have at times temporarily dammed the Stillaguamish River and diverted the channel considerably southward. These riverside events at the toe of the landslide deliver a considerable volume of fine material to the river channel and create bank deposits that erode rapidly. Several small, groundwater-fed streams drain the body of the landslide. Slumps along these stream channels form a chronic source of fine sediment to the Stillaguamish River (Shannon and Associates, 1952). Landslide activity extends a considerable distance upslope from the river edge and involves multiple blocks in various stages of evolution. Headward growth typically occurs via a series of rotational and translational slumps that expose steep head scarps in the outwash sands and have slip surfaces extending into the underlying lacustrine deposits. These slumps typically evolve downslope into mud flows. Movement tends to be slow, although rapid translation of large slumps has also occurred. Rates of movement vary over the landslide and tend to be punctuated, with the locus of activity shifting in space and time.

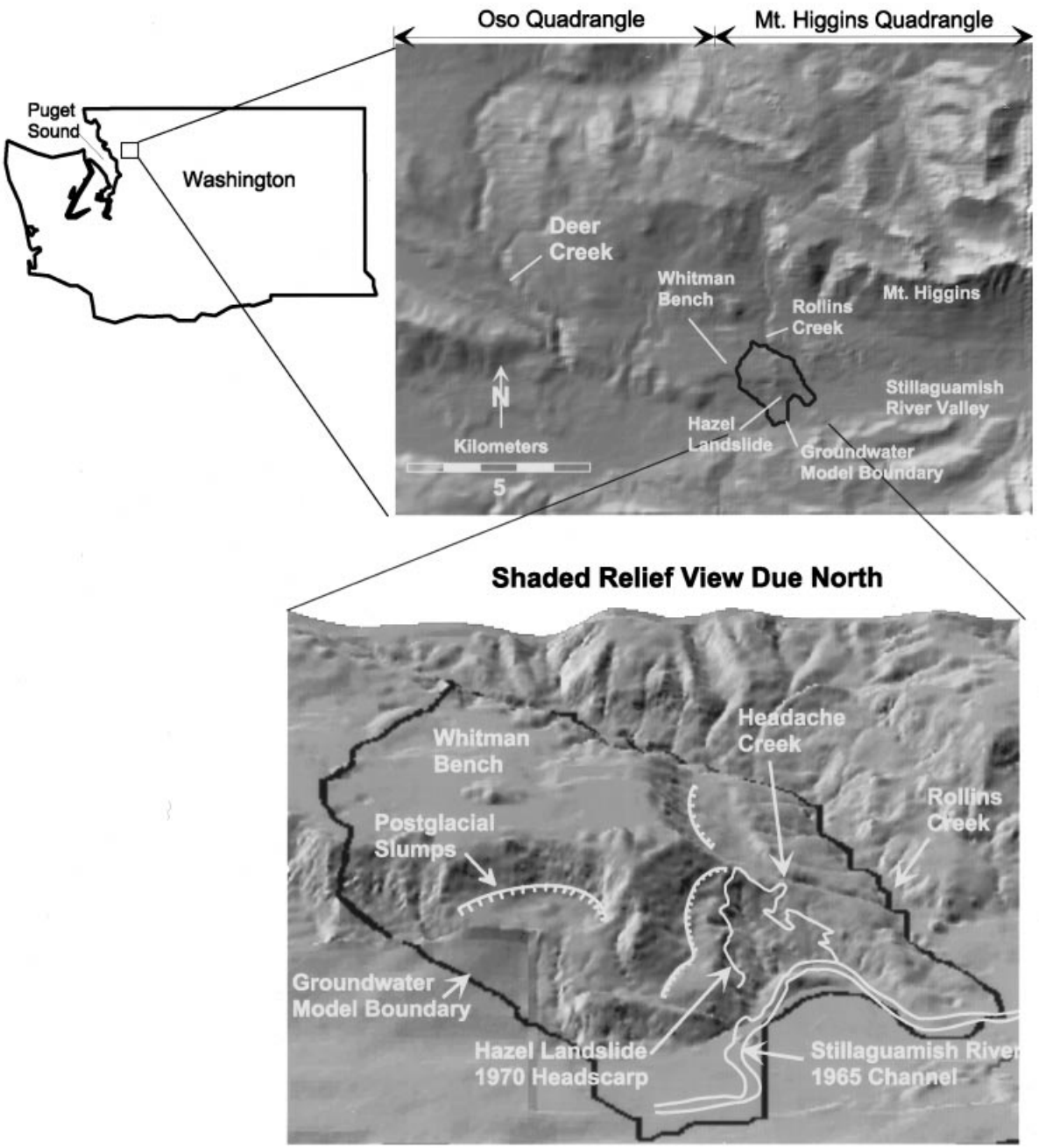

Figure 1. Location and site topography of the Hazel Landslide. The upper, shaded-relief image is created from US Geological Survey 30-m grid DEMs for the Oso and Mt Higgins 7½ minute quadrangles; the lower image is created from a 10-m grid DEM interpolated from 20-foot contour lines on a 1:4800-scale topographic map

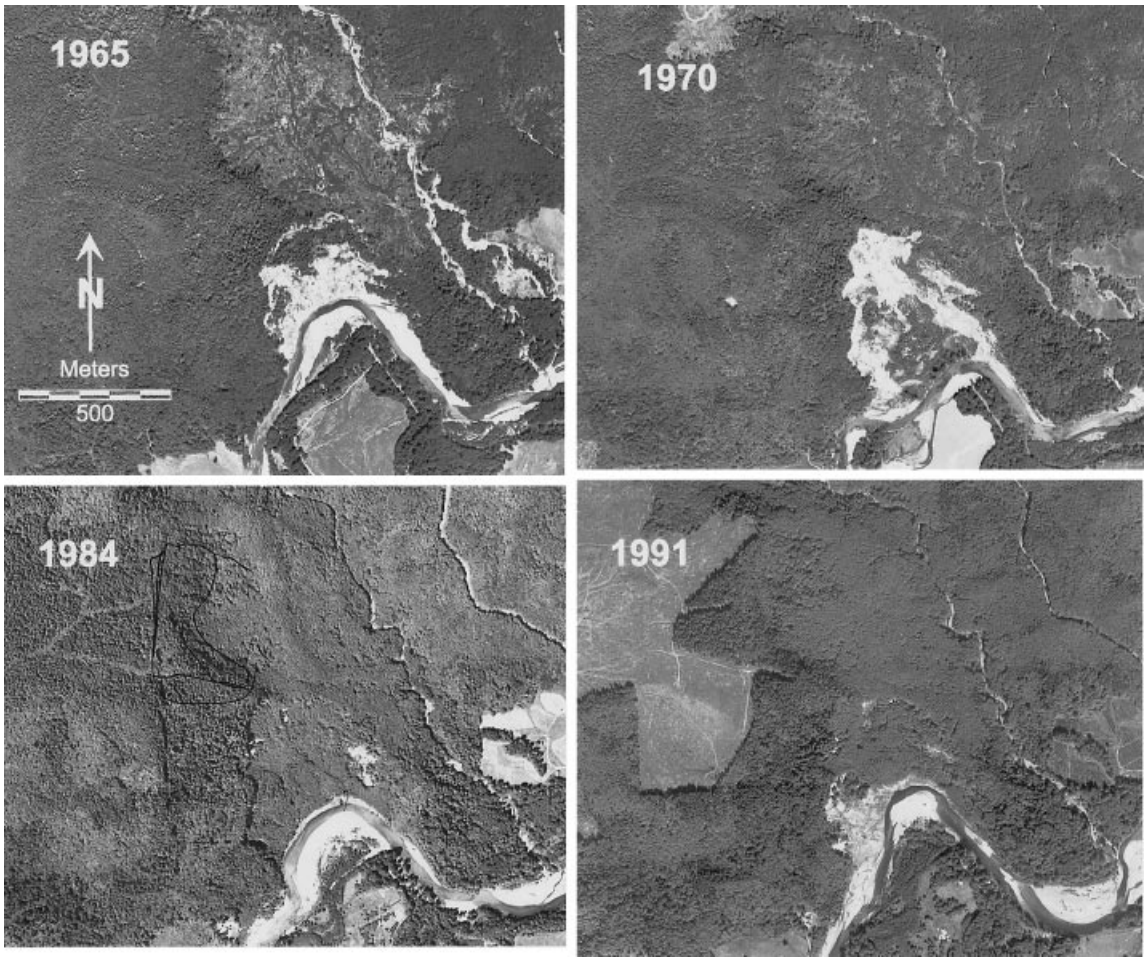

Figure 2. Aerial photography showing the landslide and vicinity. Large slump blocks and downslope flows are visible in the 1965 photograph. Also note the recent timber harvest of the small Headache Creek basin north of the landslide in this photo. A large event in 1967 dramatically altered the surface topography of the landslide and pushed the Stillaguamish River channel to the south, as seen in the 1970 photograph. The landslide scar revegetated over time, but several upslope areas exhibited persistent activity, seen as exposed soil in the 1984 photograph (the marks on the original have no bearing on this discussion). Harvest on the Whitman Bench and renewed slumping along the toe over the west end of the landslide are visible in the 1991 photograph

MODELS

With a GIS we create a spatially explicit representation of the topography and stratigraphy for the area surrounding the Hazel Landslide. Topography, illustrated in Figure 1 with shaded relief images, is represented by a digital elevation model (DEM) consisting of elevation values over a regular square grid of points (a 10 m grid spacing was used for this study) interpolated from 20-foot (6·1 m) contours on the 1 : 4800-scale topographic map. Stratigraphy is represented over the same grid with estimated elevations of the sand–clay contact, which is down-dropped in places by large slump blocks. Overlain on this landscape model are vegetation cover and precipitation values, both of which may vary in space and time. A hydrological model estimates groundwater recharge at each grid point as a function of vegetation cover, precipitation and

temperature. The grid defines a finite-element mesh for a groundwater model, with recharge values over the grid specifying groundwater influx. Calculated water table elevations specify head values at each grid point, which are used in calculations of slope stability. Factors of safety are calculated along linear slope transects to estimate the minimum stability for every grid point. We then alter the vegetation cover to represent timber harvest (or alter the topography to represent bank erosion or channel incision) and repeat the exercise to find the relative decrease in stability at each point occurring in response to the applied change.

There is a vast range of hydrological, groundwater and slope stability models from which to choose. We are restricted by the data and resources at our disposal. Available data do not include geotechnical tests, water table elevations or extensive subsurface investigations, so we must keep the required number of model parameters to a minimum. This is an exploratory analysis intended, in part, to evaluate the necessity of further study, so low cost is another goal. We therefore selected inexpensive software to run on personal computers. The GIS we use is IDRISI (Clark Labs, 1997); the other models are described briefly below and in greater detail in Miller and Sias (1997).

Hydrology

Empirical paired catchment studies provide some indication of the magnitude of the change in recharge that occurs following timber harvest (Bosch and Hewlett, 1982; Stednick, 1996). These studies, however, show that site-specific factors are important determinants of the effects of timber harvest on water yield. A survey of rainfall and stream flow records in the region revealed no station pairs from which we might be able, at least roughly, to estimate the average annual evapotranspiration for a small forested and a small deforested catchment having zonal climate and geology similar to that of Hazel.

Faced with the task of estimating annual and, for transient analyses, shorter term recharge without the benefit of suitable paired catchment rainfall–runoff data, we chose to perform a hydrological simulation using a model adapted from Kelliher *et al.* (1986). These authors used the Penman–Monteith equation (Monteith, 1965) to estimate growing season evapotranspiration (ET) for a 31-year-old thinned Douglas fir stand on eastern Vancouver Island, British Columbia, Canada. This and numerous other studies (e.g. Rutter *et al.*, 1971; McNaughton and Black, 1973) have demonstrated that, for a wide variety of climates and vegetation covers, the Penman–Monteith equation can provide reasonably good estimates of growing season ET using *a priori*-determined soil and vegetation parameters. In particular, the study by Kelliher *et al.* (1986) shows that good results can be obtained for a Pacific Northwest coniferous forest.

The modified model uses a simplified representation of soil hydraulics (a so-called bucket model). The only required soil properties are the soil moisture content at field capacity and permanent wilting point. Soils (glacial sediments) at the Hazel site are deep and well drained, and the terrain is level over the majority of the groundwater recharge area; therefore, we did not include overland flow and lateral shallow subsurface flow in the model. Under these conditions, estimation of recharge as a function of vegetation cover reduces to a problem of estimation of evapotranspiration.

The model parameters are listed in Table I. Because we are interested in the effect of end-member vegetation cover on recharge, the model parameters are all vegetation dependent. As field determination of vegetation parameters was not feasible, we estimated from the literature what we consider to be reasonable upper and lower parameter bounds for a 'typical', non-species-specific coniferous forest (i.e. 20–40 m tall, single-layer, closed canopy) and a revegetated clear-cut (i.e. having a short, deciduous canopy and no overstorey) in the Pacific Northwest region. Model parameter values are given in Table I. For application to winter (October–March), leaf area index (LAI) was assumed to fall to nearly zero for the clear-cut and to decrease slightly for the forest. All other vegetation parameters are seasonally invariant.

Uncertainty as to the values to assign to the vegetation parameters in the evapotranspiration model translate to uncertainty in calculated recharge. For each cover, a high and low estimate for recharge was obtained by setting all parameters to their lower and upper bounds, respectively [parameters were defined such that upper (lower) bound values corresponded to high (low) evapotranspiration rates]. Climate was assumed invariant with changes in vegetation.

Table I. Model parameters, upper and lower parameter bounds and intermediate values

Parameter	Units	Evergreen forest			Clear-cut	
		Lower	Middle	Upper	Lower	Upper
r_a	s/cm	0·1	0·07	0·04	0·3	1·2
r_s-min	s/cm	2·5	2·5	2·5	2·0	1·5
LAI	m^2/m^2	5	7	10	0·75	1·50
FTHRU	Dimensionless	0·8	0·70	0·65	0·90	0·80
RZ-max	mm	200	250	300	100	150

r_a, aerodynamic resistance; r_s-min, minimum stomatal resistance; LAI, leaf area index; FTHRU, fraction throughfall plus stemflow; *RZ*-max, maximum root zone storage (storage at field capacity)

Evapotranspiration was calculated at a 6-hour time-step, as better results are obtained with the Penman–Monteith equation when the diurnal cycle is represented (McNaughton and Black, 1973). Six-hour meteorological variables (vapour pressure deficit, net radiation and air temperature) were inferred from daily precipitation and daily minimum and maximum temperature (T_{min} and T_{max}). Daily rainfall amounts were treated as 18-hour storms of constant intensity (on rainy days, the period 6 p.m. to midnight was taken to be rain free). We used a sinusoidal function to represent the diurnal variation in air temperature, the method of Running *et al*. (1987) to estimate vapour pressure deficit from T_{min} and T_{max}, and the algorithm of Bristow and Campbell (1984) to estimate daily insolation. Albedo was taken to be 0·12 and 0·18 for forest and clear-cut, respectively (Running *et al*., 1987). Long-wave radiation, based on air temperature and climatological averages of monthly cloud cover, was assumed to be constant over each 24-hour period, whereas insolation was assumed to be zero from 6 p.m. to 6 a.m. throughout the year. Because wind speed data were unavailable, aerodynamic resistance was treated as a vegetation parameter. Further details regarding the hydrological model (structure, parameter determination, elaboration of forcing data) can be found in Miller and Sias (1997).

Groundwater

We used MODFE, a groundwater model written by and available from the US Geological Survey. The program is freely available (Torak, 1993a; also over the internet at http://h2o.usgs.gov/software), well documented (Cooley, 1992; Torak, 1993b) and has a history of use (Czarnecki and Waddell, 1984; Buxton and Modica, 1992; Iverson and Reid, 1992; Reid and Iverson, 1992; Torak *et al*., 1992). MODFE is a two-dimensional finite-element model using linear, triangular elements. It can simulate both steady-state and transient groundwater flow in confined or unconfined aquifers and can accommodate seepage at the ground surface. We used the program to simulate unconfined aerial groundwater flux and to calculate water table elevations.

To represent aerial groundwater flux, the program assumes horizontal flow. The aquifer is characterized in terms of horizontal transmissivity, a measure of the potential horizontal flux of groundwater below a point on the ground surface, and specific yield, a measure of the change in volume of water stored within the aquifer caused by a unit change in water table elevation. Transmissivity is calculated as the depth integration of saturated hydraulic conductivity. In its original form, MODFE assumes a vertically homogeneous aquifer. For use at the Hazel Landslide site we modified the calculation of transmissivity to accommodate multiple layers.

The data required to describe the aquifer for this model are: (1) elevation of the ground surface; (2) elevation of stratigraphic contacts separating materials having differing hydraulic conductivity; and (3) hydraulic conductivity and specific yield for each of the materials. Ground surface elevations to construct a DEM are obtained from topographic mapping. Stratigraphic contacts and material properties of the aquifer had to be estimated. Stratigraphy was inferred from field-mapped contacts and surface morphology.

Surface groundwater seeps also proved useful for estimating contact locations. Hydraulic conductivity and specific yield values are constrained to some extent by the soil and rock types present. These values were adjusted during calibration runs of the model so that surface seepage is predicted in the same localities as observed. All data values are specified over a square grid of points within the GIS (IDRISI) and may vary spatially. We wrote pre- and post-processors using the IDRISI data structure so that MODFE was run directly from IDRISI files.

The grid points served as nodes of the finite-element mesh. A zero-flux boundary condition is enforced on the upslope boundary of the mesh, causing it to act as a water table divide. The upslope boundary was positioned along the drainage divide inferred from surface topography. In test runs of the program, the boundary was moved slightly to ensure that its location had no effect on calculated head values in the vicinity of the landslide. The remaining portions of the mesh boundary were positioned along a stream channel to the side of the landslide (Rollins Creek in Figure 1) and along the Stillaguamish River at its base, both inferred to be effluent from field observations of year-round seepage at their banks. Fixed-head boundary conditions were enforced along these portions of the mesh boundary.

Recharge values were specified for all interior nodes of the mesh. For a given pattern of recharge, the model calculates head elevations for all nodes. These elevations define a water table surface. Discharge values, to simulate seepage, were specified wherever the water table was at the ground surface (no recharge occurs at those nodes). A steady-state analysis produces a single water table surface corresponding to continuous recharge constant over time; a transient analysis produces a water table surface for each time step and illustrates aquifer response to changes in recharge over time. The head values are used by the stability model described below and to determine groundwater flow directions, from which the recharge area to specific points can be delineated.

The aerial extent of the recharge area must be inferred from model results. The calculated water table elevations were used with algorithms described in Jenson and Domingue (1988) for determining flow direction and delineating watersheds. The groundwater divide located for drainage to the landslide delineates the recharge area (Figure 3). We found that the spatial extent of the estimated recharge area varied little with temporal changes in recharge. We did not examine the effects of spatial variations in recharge.

Slope stability

Large landslides often exhibit a variety of mass-wasting processes. For example, the Hazel Landslide has experienced large slumps with rapid movement over a relatively planar slip surface. It also contains many rotational slumps of varying size, some of which fail catastrophically and some of which move incrementally year by year. Slump blocks may remain relatively coherent, with intact stratigraphy, others disintegrate into flows.

No single model can accurately portray all these types of behaviour, so, instead of a detailed landslide representation, we rely on a simple characterization of the potential for downslope mass movement. Gravity acts to move material downslope; movement is resisted by material shear strength. We estimate the relative magnitude of these forces by assuming limit equilibrium along distinct slip surfaces, using Bishop's simplified method of slices (Bishop, 1955) to calculate a factor of safety along individual slope transects. This procedure ignores the process of mass movement and focuses instead on the potential for movement.

We make no prior assumptions about the location of potential slip surfaces. For each slope transect, we use numerical minimization to find the set of slip surfaces giving the lowest factor of safety for each point along the transect (described in Miller, 1995). This procedure produces a 'factor of safety' profile, as shown in Figure 4. Each transect entails a multitude of potential slip surfaces; each slope entails a multitude of potential transects. We construct a linear transect from every grid point, oriented parallel to the slope aspect at that point and extending the length of the project area. Each grid cell (a cell is the surface area associated with a grid point) is thus intersected by numerous transects. Each point is assigned the lowest factor of safety found within its cell area. This procedure estimates the aerial pattern of relative slope stability.

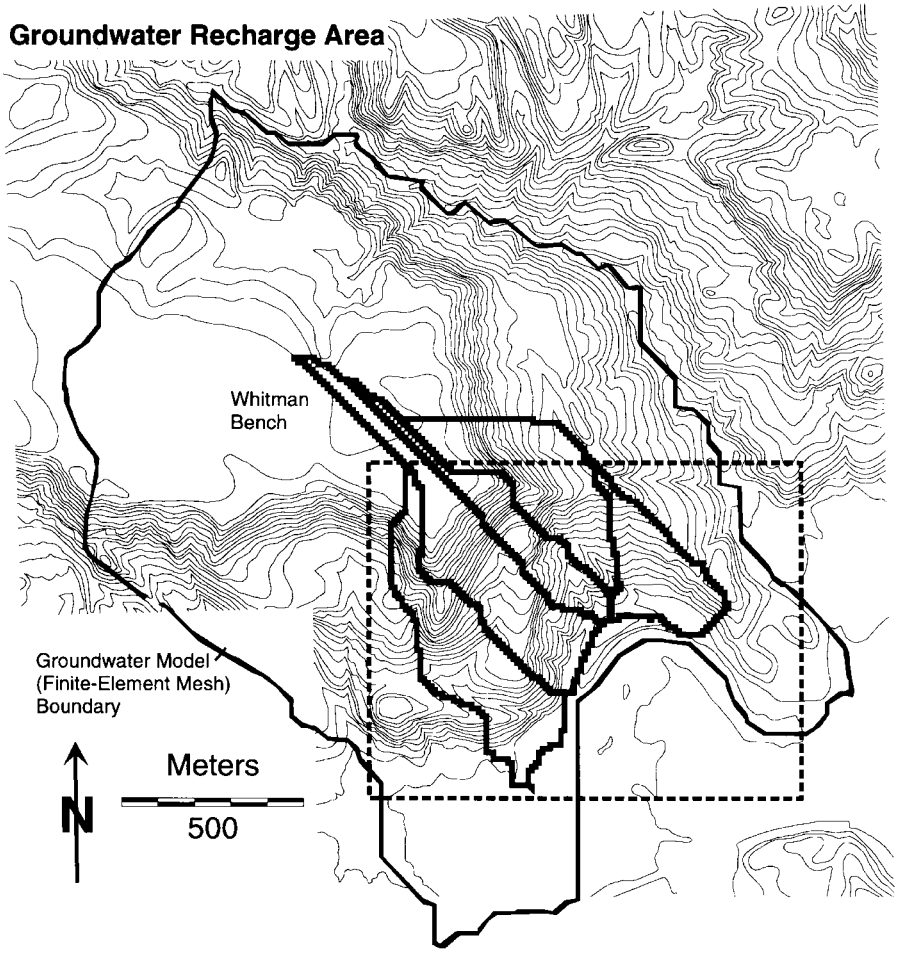

Figure 3. Estimated groundwater recharge area of the landslide. Heavy lines outline adjacent polygons that delineate five distinct zones of groundwater flow to the landslide, based on a steady-state simulation for fully forested conditions. The dashed rectangle outlines the area shown in Figures 4 and 6

The use of Bishop's simplified method of slices entails a circular slip surface and horizontal interslice forces. This method is numerically robust, which is why we use it, but it does not represent the least-stable geometry as well as other methods may (see, for example, Duncan and Wright, 1980). A circular shape still provides a great range of slip surface locations to examine, since the radius may vary to infinity. We do include a planar surface in the minimization scheme. A vertical tension crack is also allowed at the head scarp in every case. The depth of the tension crack is an adjustable variable in the search for the minimum factor of safety. We have experimented with other geometries. Spencer's method (Spencer, 1967) required a fourfold increase in processing time, and produced slightly lower factor of safety values in some areas. The relative change in the predicted factor of safety for different scenarios was, however, negligibly different from that obtained with Bishop's method.

We use a two-dimensional model, which implies plane strain (in the vertical plane). Extension of these methods to a three-dimensional analysis, although feasible (e.g. Hungr, 1987), is beyond our computing capacity. In general, a three-dimensional analysis produces larger factor of safety estimates than a two-dimensional analysis (see review, Duncan, 1992). We are unsure, however, of how three-dimensional effects would change the computed change in the factor of safety for different scenarios. In our current scheme, the

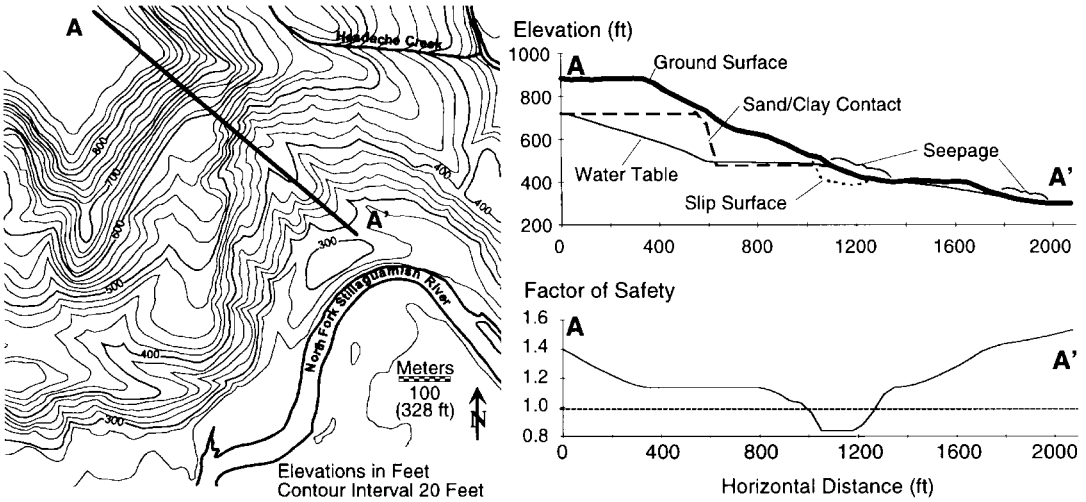

Figure 4. One transect used for calculating slope stability. Elevations of the ground surface, underlying stratigraphic contacts and water table are interpolated at equal intervals (10 m) from GIS grid files. These data are used to find the radius of the least-stable slip surface between every combination of interpolation points, from which the stability of the slope is estimated for each point along the transect, shown in the lower graph. The least stable slip surface found along this transect is shown in the upper graph. Thousands of such transects are used to estimate spatial patterns of slope stability

stability estimates for adjacent points along a slope contour are in no way connected; a three-dimensional analysis would include such interactions. We expect that a two-dimensional analysis, in some cases, underestimates the aerial extent of slope response and overestimates its magnitude.

The data required are: (1) ground surface elevations; (2) stratigraphic contact elevations; and (3) property values (cohesion, angle of internal friction and saturated and moist bulk densities) for each material. Determination of surface elevations and stratigraphic contacts was discussed in the description of the groundwater model above. Because these methods are intended for areas having little or no geotechnical data, material properties must be estimated. The rock and soil types present broadly limit the range of potential values. Specific values must be chosen through back-calculation over selected slope transects. We examined transects on both apparently stable and actively failing slopes that traversed all the stratigraphic units present (sand and clay). Using groundwater head values obtained for a typical wet season, we sought a combination of property values that produced factors of safety greater than 1 for stable slopes and less than 1 for failing slopes. The final values are reported in Table II.

We were not entirely successful in finding a single combination of property values appropriate for every slope examined. Material heterogeneity, particularly within a single stratigraphic unit, makes such success unlikely. The difference between peak and residual strengths can be large. [Palladino and Peck (1972) in examination of a deposit similar to that found at the Hazel site, report a peak strength represented by a cohesion of 0·65 ton/ft^2 (62 kPa) and a friction angle of 35° for intact clay, compared with a residual strength

Table II. Geotechnical properties

Property	Outwash sands	Lacustrine clays
Saturated conductivity (m/h)	0·36	0·00036
Specific yield	0·25	0·1
Bulk density (dry) (kg/m^3)	1870	2020
Bulk density (saturated) (kg/m^3)	2120	2120
Angle of internal friction (°)	38	23
Cohesion (kPa)	5	14

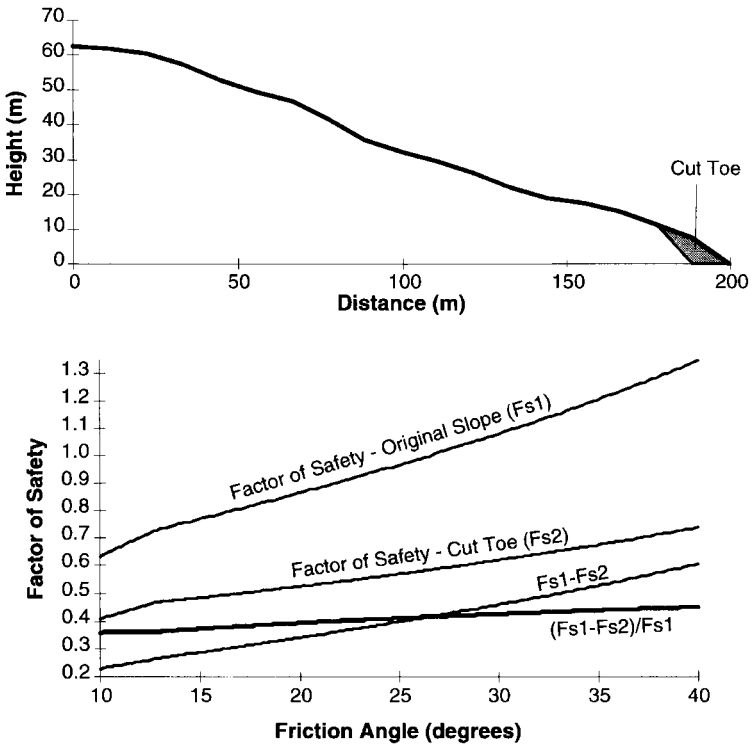

Figure 5. Proportional response as a measure of landslide sensitivity that is relatively insensitive to errors in estimated geotechnical properties

represented by a cohesion of zero and a friction angle of from 13·5 to 17·5° for disturbed clay.] The transects used for back-calculating property values traverse slopes of both disturbed and intact material. Over disturbed slopes, the depth to intact material is unknown. The values we chose are thus a compromise between peak and residual strengths, so that factors of safety for intact slopes are systematically underestimated and those for failed slopes are systematically overestimated.

Unresolved spatial heterogeneity is a confounding factor that renders predicted factor of safety values uncertain. Unfortunately, we see no means of mapping heterogeneity inexpensively (in three dimensions) at the scale of individual slump blocks. We therefore minimize reliance on factor of safety estimates by examining the change, rather than the actual values themselves, predicted for some change in a model variable. The proportional decrease in stability caused by an increase in recharge or cutting of the slope toe, for example, is relatively independent of the geotechnical values assigned to the material. This is illustrated in Figure 5, which shows the factor of safety calculated for a slope entirely in clay. Stability of the slope both before and after cutting of the toe, and the difference between these two cases, is highly dependent on the friction angle assigned to the clay. The proportional change, however, varies over a much smaller range. Hence we use the proportional change, calculated as

$$\frac{(Fs_1 - Fs_2)}{Fs_1} \tag{1}$$

(where Fs_1 and Fs_2 are the factors of safety before and after a perturbation, respectively), as an indicator of slope response that is less sensitive to errors in the assigned geotechnical properties than the factor of safety values themselves. We use Equation (1) to evaluate and compare the effects of changes in slope topography (cutting of slope toes) and changes in pore pressure (associated with changes in groundwater recharge).

Variation of pore pressures is a primary control on slope stability. We are interested in both spatial and temporal variability. Pore pressures in the model are defined by the head values obtained with the groundwater model. In using a two-dimensional groundwater model that approximates only the horizontal components of the flow field, we focus on the aerial variation in hydrostatic pressure, but miss the effect on slope stability of head gradients in the vertical plane, which are substantial on slopes and across contrasts in hydraulic conductivity (Iverson and Reid, 1992; Reid and Iverson, 1992). When examining slope response to relatively small head changes, with no change in topography, the effects of this shortcoming should be minimized by use of Equation (1). When the topography is altered by cutting of the slope toe, consequent changes in vertical components of the flow field, which are not represented here, may have a larger effect on slope response, primarily near the toe. We have not yet quantified these effects within the context of the models used here. We expect that estimates of slope response to both pore pressure changes and to alterations of slope topography are, in some areas, underestimated.

RESULTS: STEADY-STATE AND TRANSIENT ANALYSES

Groundwater recharge

For a given climatic time-series, the hydrology model provides a time varying, point estimate of recharge to groundwater as a function of vegetation cover. Although vegetation may vary both spatially and temporally within the model, we chose to examine two scenarios having vegetation attributes constant in both space and time: fully forested and fully clear-cut. More realistic harvest scenarios that include limited patches of clear-cutting and forest regrowth could be simulated; our goal here was to estimate the maximum effect of clear-cutting over any time interval throughout the climatic time-series.

The model predicts that average annual forest evapotranspiration at Hazel lies between 45 and 75% of annual rainfall, and that winter evapotranspiration accounts for 50% or more of annual evapotranspiration. This result is a consequence of above freezing winter temperatures at the Hazel site. Lower temperatures would result in less winter evapotranspiration. The predicted annual interception loss for forest ranges from 312 to 552 mm. [This prediction compares well with the results of a recent US Geological Survey study, in which annual interception loss for a Puget Sound lowland forested plot, situated on glacial till, was found to be 450 mm. Annual rainfall was about 1000 mm at that site (Henry Bauer, personal communication).] Annual evapotranspiration for the clear-cut amounts to about 20% of annual rainfall. Summer evapotranspiration is quite similar for both forest and clear-cut. Winter evapotranspiration for the clear-cut is negligible.

The difference between the forest high recharge case (923 mm/yr mean value) and the clear-cut low recharge case (1204 mm/yr) forms the low estimate for change in recharge due to clear-cutting (281 mm/yr). The difference between the forest low recharge case (512 mm/yr) and the clear-cut high recharge case (1375 mm/yr) forms the high estimate for change in recharge due to clear-cutting (883 mm/yr). The predicted change in average annual evapotranspiration owing to clear-cutting is mostly attributable to a nearly 100% decline in evapotranspiration in winter.

Landslide response to harvest-related increases in recharge

We used the time-averaged recharge values for the fully forested and fully clear cut scenarios with the groundwater model to estimate steady-state head values for each case. The estimated recharge area to the landslide varied negligibly between the two. The change in landslide stability was gauged for each point over the landslide using Equation (1). Because of uncertainty in the vegetation parameter values, this exercise was performed for both the smallest and largest estimated changes in recharge. The results are shown in Figures 6A and 6B.

High sensitivity to increases in recharge does not necessarily indicate that the landslide will be affected. A stable, but sensitive, slope will be stable in either case (and vice versa). Thus, grid points predicted to be

stable, as defined by a factor of safety of 1·3 or greater in the least stable case [Fs_2 in Equation (1)], are excluded from these maps.

The resulting maps of sensitivity indicate that certain portions of the landslide respond to changes in recharge differently than do other portions: many areas are unaffected, while others experience up to a 30% decrease in stability. The pattern revealed is a consequence of: (1) the spatial differences of the change in head values over the landslide between forested and clear-cut conditions; and (2) the spatial variability of surface and subsurface geometry, which produces a unique response from each slope to a change in head.

Despite our use of spatially invariant vegetation attributes for these analyses, one may use these results to estimate spatial correlations between areas of recharge and landslide response. Compare the pattern of sensitivity shown in the maps of Figure 6 with the recharge zones delineated for various portions of the landslide in Figure 3. Different parts of the landslide are fed by separate recharge zones; hence, a change in vegetation through a portion of the recharge area, a harvest unit for example, should primarily affect only a certain portion of the landslide.

Response to cutting of the slope toe

To evaluate the effects of bank erosion at the toe, we simply 'removed' material from the model and moved the northern river edge to its approximate 1984 location. We then recalculated the factors of safety for this modified topography and used Equation (1) as a measure of the change. We used forested recharge values (high estimate) for each case. The pattern of response shown in Figure 6C is a function of the surface and subsurface geometry represented in the model.

Increased recharge and bank erosion at the toe both cause spatially variable effects, with each primarily affecting different portions of the landslide. Near the toe, bank erosion lowered the estimated stability by nearly 75%, a much larger effect than that associated with increased recharge. Upslope, the largest change is associated with increasing recharge, although the maximum indicated reduction is 30%, less than half of the maximum estimated for toe cutting.

Response to incision of channels draining the landslide

Several small streams drain the body of the landslide. Numerous adjacent slumps and persistent mud flows feed into their channels. Evidence of channel incision (noted also by Shannon and Associates, 1952) and bank-cutting suggests that mass wasting is initiated and frequently reactivated by fluvial erosion of the channels. Small-scale slumping into these channels occurs throughout the winter months, with fluvial flushing of the fine-grained debris into the Stillaguamish occurring year-round. Over time these minor topographic readjustments and the continual removal of material may act to destabilize larger portions of the landslide, thus activating larger slumps. We evaluate the effects of this process on landslide stability below.

We use the 10-m grid DEM to delineate channels on the landslide as shown in Figure 6D. Channel head locations are estimated from their current field locations. We then digitally incise every channel by one meter and recalculate factors of safety over the landslide. The effects of this incision are displayed, via Equation (1), in Figure 6D.

Discussion of steady-state analyses

Aerial photographs and previous reports (Figure 2; Shannon and Associates, 1952; Benda *et al.*, 1988) document landslide activity over the last 50 years and are summarized in Figure 7A. Topographic data for this study were based on 1978 aerial photography, so some interpretation is required in applying our results to the landslide over time. A large 1967 event dramatically altered the surface geometry of the landslide and calculated stability and sensitivity will not apply before that time. Topographic changes since 1978, such as northward migration of the river channel and slumping along the western portion of the landslide, may also alter landslide responses from those suggested in Figure 6.

Nevertheless, observed landslide activity correlates well with areas predicted to respond to one or more of the applied changes. Upslope areas of activity seen in post-1970 photographs and in the field (1995–1996)

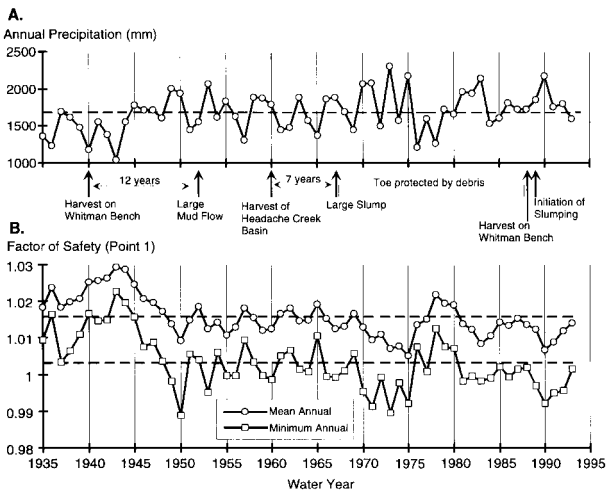

Figure 7. (A) Annual precipitation over the period of record. Timing of timber harvest and landslide activity are also indicated. (B) Estimated mean annual and minimum annual factor of safety over the period of record for point 1 in Figure 6B. Estimated slope stability varies inversely with annual precipitation, but also shows longer term variation. Stability at any time depends on the history of recharge over multiple years

fall within areas indicated to be sensitive to increases in recharge and to incision of channels draining the body of the landslide (compare light patches, indicating areas of exposed soil in the photographs, in Figure 2 with the maps in Figure 6). Large riverside slumps in 1988, and again since 1996, occurred in areas sensitive to cutting of the toe. Extensive slumping in an area sensitive to channel incision occurred during a large winter storm in 1996. The predicted pattern and relative magnitude of landslide response to these different environmental factors offer hypotheses to explain observed landslide activity.

However, many of the sensitive areas shown in Figure 6 show no signs of instability. Slopes up to the Whitman Bench, for example (the large red to yellow area in the north-western portion of Figure 6A), appear, on examination in the field, to be quite stable. The predicted high sensitivity of stable slopes is a consequence of two factors: a stable slope may experience a decrease in the factor of safety and still be stable and, because material strength parameters are underestimated for undisturbed slopes, the stability for these slopes is also underestimated. Predictions of sensitivity to change in a particular model variable can serve to elucidate field observations, but must be interpreted within the context of those observations.

Effects of toe cutting. Landslide history clearly indicates great dependence on conditions at the base along the Stillaguamish River. Big, river-moving events have occurred only when the channel impinges on the toe. No large events took place during the rather wet years of the early and mid 1970s when the toe was protected by debris from the 1967 event (Figure 7A). It was not until 1988, when that debris was eroded away and the river again had access to the toe of the landslide, that large-scale, riverside slumping reoccurred. At the base of the slope, the calculated effects of toe erosion are many times greater than those of increased recharge or channel incision, and the zones of observed activity match well with those predicted to be sensitive to toe cutting.

Even during times of apparent quiescence, however, activity persists upslope, as shown by the persistent appearance of exposed headscarps and unvegetated areas in 1978, 1984 and 1988 photographs. Several areas of upslope activity were observed during field visits in 1995 and 1996 (shown in Figure 6). In general, upslope areas of observed landslide activity correlate well with areas predicted to be sensitive either to increases in recharge and/or to incision of channels draining the landslide.

Effects of timber harvest. Benda *et al*. (1988) noted: (1) the increase of landslide activity in the early 1950s following timber harvest on Whitman Bench in 1940; and (2) the increase of landslide activity in the

mid-1960s following harvest of the Headache Creek basin in 1960. We now add, (3) slumping in the western portion of the landslide shown in the 1991 photograph following timber harvest within the groundwater recharge area on Whitman Bench in 1988.

We can compare the location of the harvest to the subsequent locus of activity on the landslide. Based on the recharge areas delineated for different portions of the landslide in Figure 3, the harvest of Headache Creek basin, as occurred around 1960, should primarily affect the east-central portion of the landslide, correlating with the location of the large 1967 event (compare the landslide scar in the 1970 photograph of Figure 2 with the polygons shown in Figure 3). Harvest of the Whitman Bench, as occurred in the late 1980s, should primarily affect slopes through the west and west-central portions of the landslide, correlating with activity in the 1990s. Model predictions suggest that logging activity in certain portions of the recharge area will affect certain portions of the landslide. Such a cause and effect relationship is not refuted by the observed spatial correlations between logging and landslide activity.

One must examine these correlations in relationship to the pattern of annual precipitation (Figure 7A). The first reported period of landslide activity (1950s) started during a year of below average rainfall. The other two periods started during years of slightly above average rainfall. The first two periods of landslide activity began 12 and 7 years after harvest, the third about a year after harvest. Interpretation of these observations requires a look at the temporal nature of landslide response.

Temporal patterns of slope response

Groundwater flux to the landslide varies over time in response to changing rates of recharge. Recharge varies both seasonally, being greater in winter than in summer, and annually, being greater in wet years than in drought years. The variability in recharge caused by annual variability in precipitation is larger than the change estimated for conversion from forested to clear-cut conditions. Any change in recharge caused by logging must be assessed in conjunction with natural year to year variability in precipitation.

The time variability of groundwater flux and consequent changes in slope stability can be simulated with the models presented here. Unfortunately, our computing capacity was insufficient to generate a factor of safety time series for all points on the landslide. It is, nevertheless, instructive to examine temporal changes at a limited number of points.

Transient groundwater simulations indicated that the aquifer responds to multiyear patterns of precipitation. A series of wet years can elevate the water table for several subsequent dry years, and vice versa. For the points examined, the calculated factor of safety varied inversely with the volume of water in aquifer storage, which varies directly with multiyear patterns of precipitation. The predicted time-series of stability, drawn for a single point in Figure 7B, shows annual variability driven by year to year changes in rainfall, overlain on longer term variability driven by multiyear patterns of rainfall.

Regression of the factor of safety to total annual precipitation for previous years indicates that slope stability at this point responds to the previous five years of precipitation (Figure 8). The length of this memory effect is a function of the size and shape of the recharge area and of aquifer geometry and hydraulic conductivity. Our estimates for all of these values are of uncertain accuracy, so five years may be either an under- or over-estimate. Nevertheless, this result illustrates a potentially important aspect of landslide behaviour. Slopes coupled to regional groundwater flow can respond to multiyear patterns of recharge.

Although we were only able to estimate the length of landslide 'memory' for one point on the landslide, we expect that temporal patterns of landslide response vary spatially. We examined the stability of two points over the course of a single water year, the results of which are shown in Figure 9. The graphs show cumulative factor of safety frequency distributions at each point for both forested and clear-cut cases. Both points lay near the heads of small slump blocks identified in the field. Both slumps have headscarps within the sandy outwash and extend into the lacustrine deposits. Both are associated with groundwater seeps. Greatly disrupted stratigraphy, trees growing at a variety of angles and a complete lack of conifers indicate prolonged slow movement of slump block 1. Less disruption of stratigraphy and the presence of conifers suggests less movement of slump block 2, although tree growth angles still indicate a long history of movement. Despite

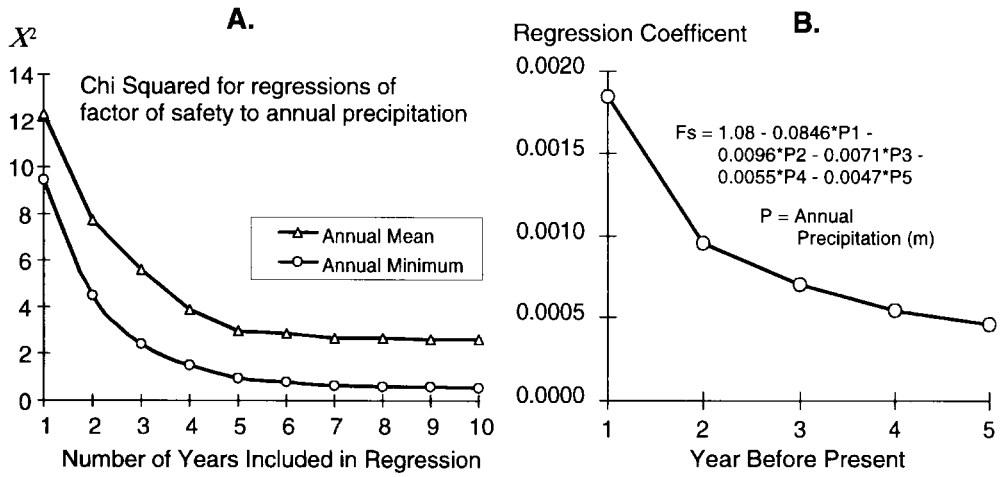

Figure 8. Stability dependence on multiyear precipitation. (A) Multiple regression of the factor of safety (at point 1 in Figure 6B) with annual precipitation. The error decreases as additional years are included in the regression, up to about five years, after which the error levels off. (B) Coefficients for the five-year regression. The current year has the greatest individual effect, but the previous four years have an overall greater influence

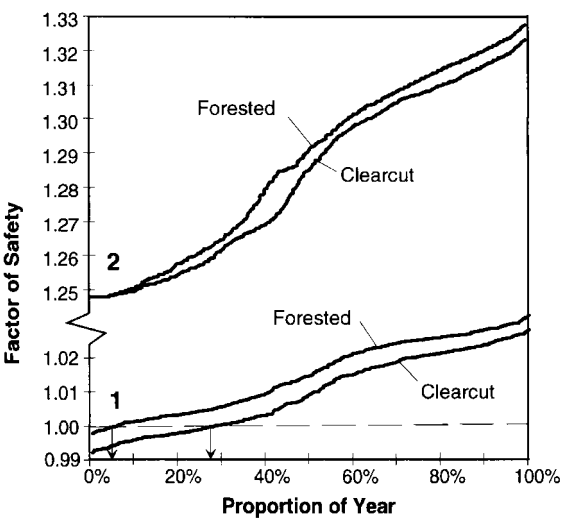

Figure 9. Factor of safety frequency distributions for points 1 and 2 (Figure 6B) over water year 1989. Results for both forested and clear-cut cases are shown. A small decrease in stability at point 1 increases the proportion of the year spent in a state of failure from 5% to 28%. Differences in the factor of safety values are of less importance than differences in the frequency distribution shape. Stability at point 2 varies over a greater range and responds differently to changes in recharge than that at point 1

obtaining factor of safety values always greater than unity for point 2, we surmise that both points dip below unity some years. Because of the problems with unresolved spatial variability in material properties discussed earlier, the difference in factor of safety values between the two points is of less importance to our analysis than the difference in their temporal patterns of change.

Failure in these cases entails a balance of forces that allows slow or intermittent mass movement. We surmise that the extent of movement depends not only on the frequency with which the factor of safety dips below unity, but also on the amount of time that it stays there. Any perturbation that lowers the stability of a marginally stable slope increases the proportion of time spent in a state of failure. As shown for point 1, a

decrease in stability of only half a per cent increased the proportion of the year spent in a condition of slope mass movement from 5 to 28%.

This result depends strongly on the shape of the frequency distribution. If the graph for point 1 were steeper near the point of instability, the increase would be less. Differences in predicted frequency distribution shapes for points 1 and 2 indicate that the temporal response of the landslide may vary from point to point in a manner unrelated to the magnitude of the change. The nature of the response to changing recharge also differs between the two points. The minimum at point 2 is unchanged between forested and clear-cut conditions. (This occurs because the slump block containing point 2 becomes completely saturated in both cases.) To characterize landslide behaviour in terms of mass-wasting sediment flux, we must examine both spatial and temporal patterns of slope response to changes in groundwater recharge (and/or other factors). The predicted magnitude of the response shown for the steady-state analyses in Figure 6 tell only part of the story. (We also note that the transient analysis suggests a smaller magnitude of stability reduction than indicated by the steady-state results.) These results suggest that it would be instructive to map some integrated measure of temporal response over the landslide.

Discussion of transient analyses

The various time lags observed between timber harvest in the groundwater recharge area and renewed activity on the landslide can be examined in light of the transient analyses discussed above. The dependence of predicted stability on multiyear patterns of rainfall reflect the time taken for water to travel through the aquifer. Transit times are a function of head gradients, which change over time as the aquifer drains through surface seeps and is recharged from above. A localized increase in recharge associated with timber harvest in a portion of the recharge zone will locally elevate the water table. The associated change in groundwater flow is communicated through the aquifer at a rate depending on the magnitude of the water table rise and on the hydraulic conductivity of the material. The results shown in Figure 8 suggest that it may take some years for head values to respond to changes across the aquifer, so that a lag between timber harvest and landslide response may be expected. We suspect that the response time varies spatially and temporally, depending on the spatial and temporal patterns of recharge. This study did not include a simulation of harvest history imposed on the time-series of recharge. Such an analysis may prove useful for estimating the relative response times for each case and, thereby, for better evaluating the degree to which past timber harvests were related to subsequent landslide activity. (Such an analysis would also provide a temporal test of the models, since we could compare the sequence of predicted landslide events to those observed.) All we can say at this time is that we expect some lag time between timber harvest-related increases in recharge and landslide response, and that the length of that lag may vary between cases, depending on the location of the timber harvest and on the sequence of precipitation events.

CONCLUSIONS

This study was undertaken to aid regulators and land managers in assessing the risk posed by timber harvest within the groundwater recharge area of a large landslide complex. Using GIS to link simple hydrological, groundwater and slope stability models using available data, we estimated the spatial patterns and relative magnitudes of potential landslide response to changes in three specific factors: (1) altered groundwater flow associated with timber harvest of the recharge area of the landslide; (2) bank erosion of the landslide toe; and (3) incision of channels draining the body of the landslide. Given the limitations of the models used and uncertainties in the material parameters chosen, we found it useful to examine the relative change in stability predicted for each case, rather than the factor of safety values obtained. These results were based on steady-state analyses and matched well with observed locations of landslide activity.

A transient analysis of slope stability performed for two points on the landslide illustrate temporal patterns of landslide behaviour (limited computer resources prevented a more extensive transient analysis). We find that stability varies inversely with annual precipitation, with additional dependence on precipitation

patterns extending over several years (five in the example here). We show how a small reduction in the stability of marginally stable slopes may greatly extend the length of time they are in a state of failure, which, for slow-moving slumps, may cause an increase of mass flux much larger than indicated by the proportional change in stability. The increased time spent in motion (failure) caused by a given reduction in stability may vary, however, from point to point over the landslide.

These results offer hypotheses to explain observed patterns of landslide behaviour. As such, they provided decision makers with improved understanding of the factors affecting slope stability and of the potential relationships between different processes active at the Hazel Landslide. Because of results of this study, future timber harvest plans at the Hazel site must be designed (through, for example, partial cuts, phased clear-cuts) to have no anticipated effect on landslide stability, and must include a detailed analysis showing how the harvest plan avoids such effects. Ensuing discussions led to acknowledgment of the uncertainties involved and of the potential to address these issues better with additional information. Hence, landslide, precipitation, and groundwater monitoring must also accompany any future timber harvests approved for this site.

ACKNOWLEDGEMENTS

Thanks to all involved with the Hazel Watershed Analysis team for their willingness to try a new approach to an often contentious land use issue. Paul Kennard, geologist with the Tulalip Tribes, and Bob Penhale, at the Washington Department of Ecology, in particular had the vision and tenacity to rally support for this undertaking. This paper benefitted greatly from reviews by D. R. Montgomery, K. M. Schmidt and one anonymous reviewer. Funding was provided by the Washington Department of Ecology and administered by the Tulalip Tribes.

REFERENCES

Benda, L., Thorsen, G. W., and Bernath, S. 1988. 'Report of the I.D. team investigation of the Hazel Landslide on the North Fork of the Stillaguamish River', *Report F.P.A. 19-09420*. Report to the Washington Department of Natural Resources, Northwest Region, Sedro Woolley, Washington. 13 pp.

Bishop, A. W. 1955. 'The use of the slip circle in the stability analysis of slopes', *Geotechnique*, **5**, 7–17.

Booth, D. B. 1989. *Surficial Geologic Map of the Granite Falls 15-Minute Quadrangle, Snohomish County, Washington*. US Geological Survey Miscellaneous Investigations Series, Map I-1852. USGS, United States Geological Survey, Washington, D.C.

Bosch, J. M. and Hewlett, J. D. 1982. 'A review of catchment experiments to determine the effect of vegetation changes on water yield and evapotranspiration', *J. Hydrol.*, **55**, 3–23.

Bristow, K. L. and Campbell, G. S. 1984. 'On the relationship between incoming solar radiation and daily maximum and minimum temperature', *Agric. For. Meteorol.*, **31**, 159–166.

Buxton, H. T. and Modica, E. 1992. 'Patterns and rates of ground-water flow on Long Island, New York', *Ground Water*, **30**, 857–866.

Clark Labs, 1997. *Idrisi for Windows*, Version 2·0. Clark Labs for Cartographic Technology and Geographic Analysis, Clark University, Worcester, Massachusetts.

Cooley, R. L. 1992. *A MODular Finite-Element model (MODFE) for areal and axisymmetric ground-water-flow problems, part 2 — derivation of finite-element equations and comparisons with analytical solutions*, US Geological Survey Techniques of Water Resources Investigations, Book 6, Chap. A4. USGS, Washington, D.C.

Czarnecki, J. B. and Waddell, R. K. 1984. 'Finite-element simulation of ground-water flow in the vicinity of Yucca Mountain, Nevada-California', *US Geological Survey Water Resources Investigations Report 84-4349*. USGS, Washington, D.C. 38 pp.

Dietrich, W. E., Reiss, R., Hsu, M. L., and Montgomery, D. R. 1995. 'A process-based model for colluvial soil depth and shallow landsliding using digital elevation data', *Hydrol. Process.*, **9**, 383–400.

Duncan, J. M. 1992. 'State-of-the-art: static stability and deformation analysis', in Seed, R. B. and Boulanger, R. W. (eds), *Stability and Performance of Slopes and Embankments II*, Geotechnical Special Publication 31. American Society of Civil Engineers, New York. pp. 222–266.

Duncan, J. M. and Wright, S. G. 1980. 'The accuracy of equilibrium methods of slope stability analysis', *Engng Geol.*, **16**, 5–17.

Hammond, C., Hall, D., Miller, S., and Swetik, P. 1992. 'Level 1 stability analysis (LISA) documentation for version 2.0', *General Technical Report INT-285*, US Department of Agriculture, Forest Service, Intermountain Research Station, Moscow, Idaho. p. 190.

Hungr, O. 1987. 'An extension of Bishop's simplified method of slope stability analysis to three dimensions', *Geotechnique*, **37**, 113–117.

Iverson, R. M. and Reid, M. E. 1992. 'Gravity-driven groundwater flow and slope failure potential, 1. Elastic effective-stress model', *Wat. Resour. Res.*, **28**, 925–938.

Jenson, S. K. and Domingue, J. O. 1988. 'Extracting topographic structure from digital elevation data for geographic information system analysis', *Photogramm. Engng Remote Sens.*, **54**, 1593–1600.
Kelliher, F. M., Black, T. A., and Price, D. T. 1986. 'Estimating the effects of understory removal from a Douglas fir forest using a two-layer canopy evapotranspiration model', *Wat. Resourc. Res.*, **22**, 1891–1899.
McNaughton, K. G. and Black, T. A. 1973. 'A study of evapotranspiration from a Douglas Fir forest using the energy balance approach', *Wat. Resour. Res.*, **9**, 1579–1590.
Miller, D. J. 1995. 'Coupling GIS with physical models to assess deep-seated landslide hazards', *Environ. Engng Geosc.*, **1**, 263–276.
Miller, D. J. and Sias, J. 1997. *Environmental Factors Affecting the Hazel Landslide*, Level 2 Watershed Analysis Report. Washington Department of Natural Resources, Northwest Region, Sedro Woolley, Washington.
Monteith, J. L. 1965. 'Evaporation and environment', *Symp. Soc. Exp. Biol.*, **19**, 205–234.
Palladino, D. J. and Peck, R. B. 1972. 'Slope failures in an overconsolidated clay, Seattle, Washington', *Geotechnique*, **22**, 563–595.
Pearce, A. J., Gash, J. H. C., and Stewart, J. B. 1980. 'Rainfall interception in a forest stand estimated from grassland meteorological data', *J. Hydrol.*, **46**, 147–163.
Reid, M. E. and Iverson, R. M. 1992. 'Gravity-driven groundwater flow and slope failure potential, 2. Effects of slope morphology, material properties, and hydraulic heterogeneity', *Wat. Resour. Res.*, **28**, 939–950.
Running, S. W., Nemani, R. R., and Hungerford, R. C. 1987. 'Extrapolation of synoptic meteorological data in mountainous terrain, and its use for simulating forest evapotranspiration and photosynthesis', *Can. J. For. Res.*, **17**, 472–483.
Rutter, A. J., Kershaw, K. A., Robins, P. C., and Morton, A. J. 1971. 'A predictive model of rainfall interception in forests, 1. Derivation of the model from observations in a plantation of Corsican Pine', *Agric. Meteorol.*, **9**, 367–384.
Shannon, W. D. and Associates, 1952. *Report on Slide on North Fork Stillaguamish River near Hazel, Washington, unpublished report to the State of Washington Departments of Game and Fisheries*. 18 pp.
Sidle, R.C., Pearce, A. J., and O'Loughlin, C. L. 1985. *Hillslope Stability and Land Use*, American Geophysical Union, Washington, DC. 140 pp.
Spencer, E. 1967. 'A method of analysis of the stability of embankments assuming parallel interslice forces', *Geotechnique*, **17**, 11–26.
Stednick, J. D. 1996. 'Monitoring the effects of timber harvest on annual water yield', *J. Hydrol.*, **179**, 79–95.
Swanston, D. N., Lienkaemper, G. W., Mersereau, R. C., and Levno, A. B. 1988. 'Timber harvest and progressive deformation of slopes in southwestern Oregon', *Bull. Assoc. Engng Geol.*, **25**, 371–381.
Tabor, R. W., Booth, D. B., Vance, D. A., and Ford, A. B. 1988. *Geologic Map of the Sauk River 30- by 60-Minute Quadrangle, Washington*. US Geological Survey Open File Report 88-692. United States Geological Survey, Washington, D.C. 50 pp., 1 map sheet.
Thorsen, G. W. 1989. 'Landslide provinces in Washington', in Galster, R. W. (ed.), *Engineering Geology in Washington*, Volume 1, Bulletin 78. Washington Division of Geology and Earth Resources, Department of Natural Resources. Olympia, Washington. pp. 71–89.
Torak, L. J. 1993a. *A MODular Finite-Element model (MODFE) for areal and axisymmetric ground-water-flow problems, part 1 — model description and user's manual*, US Geological Survey Techniques of Water Resources Investigations, Book 6, Chap. A3. USGS, United States Geological Survey, Washington, D.C.
Torak, L. J. 1993b. *A MODular Finite-Element model (MODFE) for areal and axisymmetric ground-water-flow problems, part 3 — design philosophy and programming details*, US Geological Survey Techniques of Water Resources Investigations, Book 6, Chap. A5. USGS, United States Geological Survey, Washington, D.C.
Torak, L. J., Davis, G. S., Herndon, J. G., and Strain, G. A. 1992. 'Geohydrology and evaluation of water-resource potential of the upper Floridan aquifer in the Albany area, southwestern Georgia', *US Geological Survey Water-Supply Paper 2391*. USGS, United States Geological Survey, Washington, D.C. 59 pp.
Varnes, D. J. 1978. 'Slope movement types and processes', in *Landslides — Analysis and Control*, National Academy of Sciences Transportation Research Board Special Report 176, Chap. 2. National Research Council, Washington, DC.
WDNR (Washington Department of Natural Resources), 1996. *Level 1 Hazel Watershed Analysis, Washington State*, Watershed Analysis Report, Washington Department of Natural Resources, Northwest Region, Sedro Woolley.
WFPB (Washington Forest Practices Board), 1995. *Standard Methodology for Conducting Watershed Analysis*, Version 3.0. Washington Forest Practices Board, Olympia, Washington.
Wolff, N., Nystrom, M., and Bernath, S. 1989. *The effects of partial forest-stand removal on the availability of water for groundwater recharge*, unpublished report, Washington Department of Natural Resources, Northwest Region, Sedro Woolley. 14 pp.

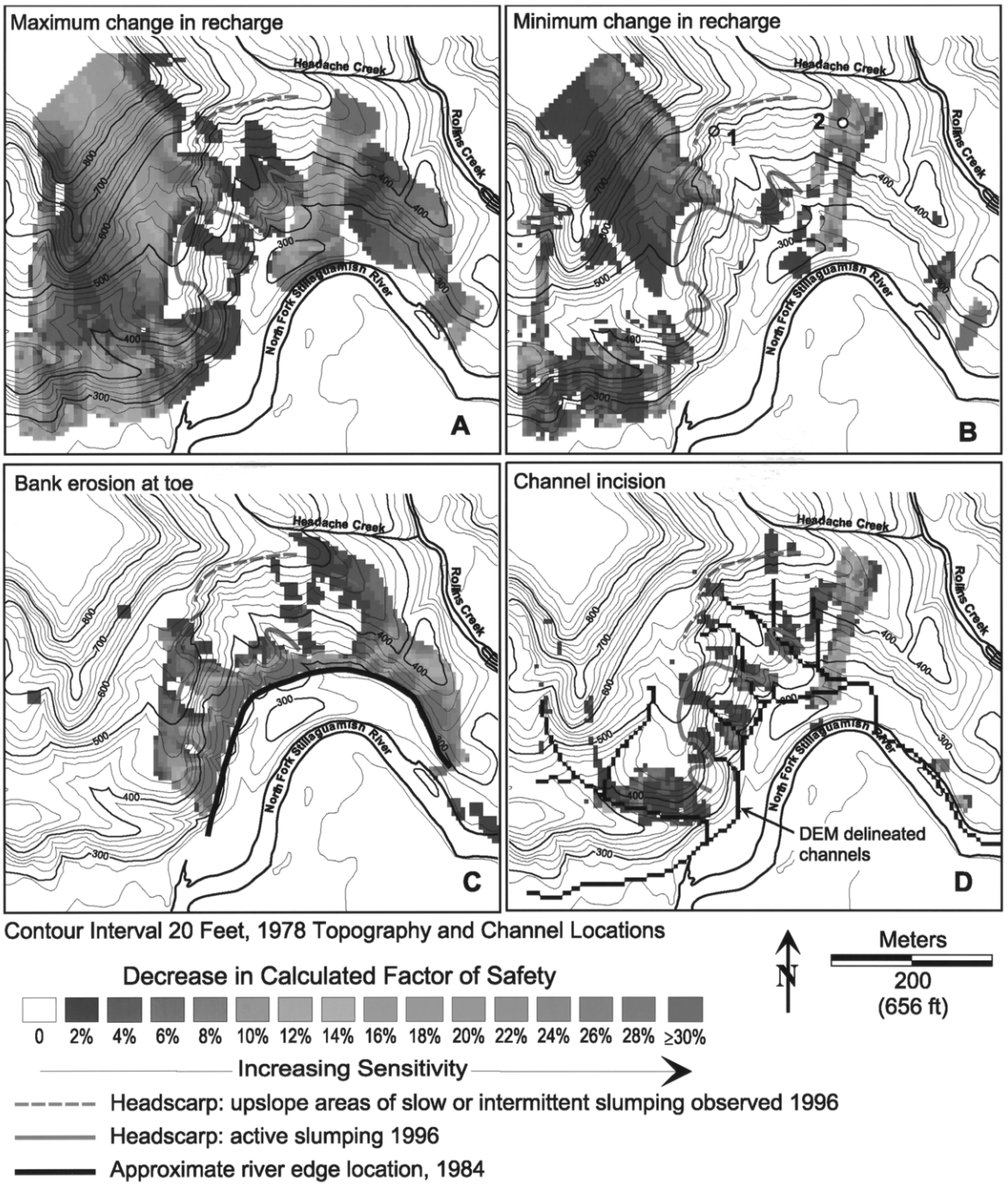

Figure 6. Changes of slope stability in response to (A) clear-cut timber harvesting of the groundwater recharge area, maximum estimate, (B) clear-cut timber harvesting of the groundwater recharge area, minimum estimate, (C) bank erosion of the landslide toe, and (D) incision of channels draining the body of the landslide. Zones of landslide activity observed during field visits in 1995 and 1996 are indicated by heavy brown lines. Points 1 and 2 shown in (B) are the locations of the transient stability analyses. Topography and channel locations are based on 1978 aerial photography